

Energy and system size dependence of chemical freeze-out in relativistic nuclear collisions

F. Becattini

Università di Firenze and INFN Sezione di Firenze, Florence, Italy

J. Manninen

University of Oulu, Oulu, Finland

M. Gaździcki

Institut für Kernphysik, Universität Frankfurt, Frankfurt, Germany and Świetokrzyska Academy, Kielce, Poland

(Received 16 November 2005; published 19 April 2006)

We present a detailed study of chemical freeze-out in p - p , C-C, Si-Si, and Pb-Pb collisions at beam momenta of 158A GeV as well as Pb-Pb collisions at beam momenta of 20A, 30A, 40A, and 80A GeV. By analyzing hadronic multiplicities within the statistical hadronization model, we studied the parameters of the source as a function of the number of participating nucleons and the beam energy. We observe a nice smooth behavior of temperature, baryon chemical potential, and strangeness under-saturation parameter as a function of energy and nucleus size. Interpolating formulas are provided which allow us to predict the chemical freeze-out parameters in central collisions at center-of-mass energies $\sqrt{s_{NN}} \gtrsim 4.5$ GeV and for any colliding ions. Specific discrepancies between data and the model emerge in particle ratios in Pb-Pb collisions at beam energies between 20A and 40A GeV which cannot be accounted for in the considered model schemes.

DOI: [10.1103/PhysRevC.73.044905](https://doi.org/10.1103/PhysRevC.73.044905)

PACS number(s): 12.40.Ee, 25.75.Dw

I. INTRODUCTION

The main goal of the ultrarelativistic nucleus-nucleus (A - A) collisions program is to create in terrestrial laboratories a new state of matter, the quark-gluon plasma (QGP). The existence of this phase, where quarks and gluons are deconfined, i.e., they can freely move over several hadronic distances, is a definite prediction of quantum chromodynamics (QCD). In the search for QGP, signals in nucleus-nucleus collisions at different nucleon-nucleon center-of-mass ($\sqrt{s_{NN}}$) energies have been studied: from few GeV at the alternating-gradient synchrotron (AGS) to several hundred GeV recently attained in Au-Au collisions at BNL's Relativistic Heavy Ion Collider (RHIC).

One of the main results is the surprising success of the statistical-thermal models in reproducing essential features of particle production [1]. This model succeeds also in describing particle multiplicities in many kinds of elementary collisions [2], suggesting that statistical production is a general property of the hadronization process itself [2,3]. Furthermore, the statistical hadronization model (SHM) supplemented with the hydrodynamical expansion of the matter, to a large extent, also reproduces transverse momentum spectra of different particle species [4].

Hence, the SHM model proves to be a useful tool for the analysis of soft hadron production and particularly the study of strangeness production, whose enhancement has long since been proposed as a signature of QGP formation. Furthermore, anomalies in the energy dependence of strangeness production have been predicted [5] as a signature of deconfinement and have been indeed observed experimentally [6].

In a recent paper of ours [7], we studied these topics in detail, comparing different versions of the statistical model. More recently, new experimental results [8] became available of hadronic multiplicities at the top super proton synchrotron

(SPS) beam energy (i.e., 158A GeV, corresponding to $\sqrt{s_{NN}} = 17.2$ GeV) in light ion collisions (C-C and Si-Si), as well as in Pb-Pb collisions at beam energies of 20A and 30A GeV (corresponding to $\sqrt{s_{NN}} = 6.2$ and 7.5 GeV, respectively). The Pb-Pb data have been recently analyzed [9] within a version of the statistical model including a light-quark nonequilibrium parameter γ_q . In the present work, we study the energy and system size dependence of chemical freeze-out by performing a systematic analysis of the available data within a more essential framework of the SHM, including only the strangeness under-saturation parameter γ_S . With the updated data sample, we also test a two-component version of the SHM, where particle production stems from the superposition of fully chemically equilibrated fireballs and single nucleon-nucleon collisions; we also briefly address, once again, the issue of whether the nonequilibrium factor γ_q is allowed.

The paper is organized as follows: a brief discussion on the SHM is given in Sec. II. In Sec. III, the experimental data selected for the analysis and the results of the analysis in our main and alternative schemes of the SHM are given. In Sec. IV, we present and discuss the energy and system size dependence of the chemical freeze-out stage. A general discussion of our results and the observed deviations from the data is given in Sec. V. Conclusions are drawn in Sec. VI.

II. THE STATISTICAL HADRONIZATION MODEL IN HEAVY ION COLLISIONS

The statistical hadronization model has been described in detail elsewhere [7]. Here, we briefly summarize its founding concepts and discuss the issue of full phase space versus midrapidity analysis.

The main idea of the statistical hadronization model is that hadrons are formed in statistical equilibrium within extended excited regions called *fireballs* or *clusters*. Several fireballs or clusters are produced in a single collision as a result of a dynamical process, each having a definite total momentum, charge, and volume.

In principle, the overall particle multiplicity should be calculated by adding those relevant to single clusters and folding with the probability distribution of volumes, masses (being Lorentz invariants, they are independent of cluster momenta), and charges. Unfortunately, this calculation is not possible within the SHM alone, because fluctuations of volumes, charges, and masses of clusters, being governed by the previous dynamical process, are not known. However, if they happen to be the same as those relevant to the random partitioning of one large cluster—defined as the *equivalent global cluster* (EGC) with a volume that is the sum of all cluster rest-frame volumes—then the overall particle multiplicities turn out to be simply those of the EGC [7], which has charges equal to the sum of single cluster charges in compliance with conservation laws. The straightforward consequence of such an assumption is that in order to calculate full phase space mean multiplicities, one can use a simple single-cluster (i.e., the EGC) formula. Of course, this is just a phenomenological simplifying assumption, and it should *not* be expected to be fully true; deviations from this simple picture should show up as second-order deviations between data and model.

It is very important to emphasize that the EGC picture takes advantage of the independence of particle multiplicity (as well as any other Lorentz scalar) on cluster momenta and, consequently, on any dynamical charge-momentum correlation. This means that the hypothesis of the single EGC calculation may hold even if clusters with large baryon number (and density) are likely to have large rapidity.

To show this in simplest terms, let us consider events with N clusters and let $w(Q_1, y_1; \dots; Q_N, y_N)$ the probability of having the i th cluster with charge Q_i at rapidity y_i . The overall average particle multiplicity of the species j reads

$$\langle n_j \rangle = \sum_{Q_1, \dots, Q_N} \int dy_1 \dots dy_N w(Q_1, y_1; \dots; Q_N, y_N) \times \langle n_j \rangle(Q_1, y_1; \dots; Q_N, y_N), \quad (1)$$

where $\langle n_j \rangle(Q_1, y_1; \dots; Q_N, y_N)$ is the average multiplicity of the species j for a particular charge and rapidity configuration. Now, being a Lorentz scalar, $\langle n_j \rangle$ can only depend on charges, hence, in fact $\langle n_j \rangle = \langle n_j \rangle(Q_1, \dots, Q_N)$. Therefore,

$$\langle n_j \rangle = \sum_{Q_1, \dots, Q_N} W(Q_1, \dots, Q_N) \langle n_j \rangle(Q_1, \dots, Q_N), \quad (2)$$

where

$$W(Q_1, \dots, Q_N) = \int dy_1 \dots dy_N w(Q_1, y_1; \dots; Q_N, y_N).$$

Thus, in order to reduce to the simple EGC case, we have to introduce some hypothesis in the form of the *marginal* distribution of charges $W(Q_1, \dots, Q_N)$ in Eq. (2), and we do not need to deal anymore with the full distribution of charges

and rapidities w in Eq. (1); charge-rapidity correlations have disappeared.

In a different approach, used in several works, the formulas of the statistical model are assumed to apply only to the *average* (with respect to all kinds of fluctuations) fireball at midrapidity. The charge probability distribution $\omega(Q, y)$ of a fireball at rapidity y is obtained from the general w in Eq. (1) by integrating over all rapidities:

$$\omega(Q, y) \propto \sum_{i=1}^N \sum_{Q_1, \dots, Q_N} \delta_{Q, Q_i} \int dy_1 \dots dy_N \times w(Q_1, y_1; \dots; Q_N, y_N) \delta(y - y_i). \quad (3)$$

Thus, in order to perform a statistical model fit, one would need to assume only that charge fluctuations at midrapidity, i.e., $\omega(Q, 0)$, are not too large, which is apparently a less restrictive requirement than that needed to ensure the validity of the EGC approach. In order to estimate the parameters of the average central fireball, the idea then is to use particle yields and ratios measured at midrapidity rather than in full phase space. However, these yields do not single out the production from the central fireball as nearby clusters also contribute to them and, if they have quite different mean charges, one would not get the desired result. Moreover, if a single cluster was formed at rest in the center-of-mass frame, a cut on a midrapidity window ($\Delta y \approx 1$) would introduce a bias in the estimation of thermal parameters because rapidity distributions are narrower for more massive particles (see, e.g., discussion in Ref. [7]). The general effect would be an increase in the fitted temperature and strangeness under-saturation parameter γ_S , which is indeed the case in an analysis at SPS energy using midrapidity densities [10]. In fact, narrower rapidity distributions for more massive particles have been measured up to the top SPS energy ($\sqrt{s_{NN}} \sim 20$ GeV). For this approach to yield consistent results, one would need a distribution of clusters with an approximately uniform charge and energy densities over a sufficiently large rapidity region, i.e., larger than the typical width of a single cluster's particle rapidity spectrum. To show this, we start by writing the rapidity spectrum of a particle as

$$\frac{dN}{dy} = \int_{-\infty}^{+\infty} dY \rho(Y) \frac{dn}{dy}(\mu(Y), T(Y), y - Y), \quad (4)$$

where $\rho(Y)$ is the density of clusters at rapidity Y and dn/dy is the primordial rapidity spectrum of particles emitted from the cluster with rapidity Y . Changing the integration variable to $y' = y - Y$, one obtains

$$\frac{dN}{dy} = \int_{-\infty}^{+\infty} dy' \rho(y - y') \frac{dn}{dy}(\mu(y - y'), T(y - y'), y'). \quad (5)$$

If $\rho(y - y')$ is approximately constant over a rapidity range (around y) sufficiently larger than the width of dn/dy , and so are $T(y - y')$ and $\mu(y - y')$, then

$$\begin{aligned} \frac{dN}{dy} &\approx \rho(y) \int_{-\infty}^{+\infty} dy' \frac{dn}{dy}(\mu(y), T(y), y') \\ &= \rho(y) n(T(y), \mu(y)). \end{aligned} \quad (6)$$

Hence, the rapidity density turns out to be proportional to the number of particles emitted from the average cluster at rapidity y . This condition also implies that the measured dN/dy is approximately constant over the same range.

However, this necessary condition is not met at center-of-mass energies $\sqrt{s_{NN}}$ up to 20A GeV, as measured rapidity distributions have a width not much larger than those from a single cluster at the kinetic freeze-out. For instance, for pions at the top SPS energy, the expected dispersion of the central cluster's rapidity distribution at a kinetic freeze-out temperature of $T \approx 125$ MeV is about 0.8, while the dispersion of the actual distribution is ≈ 1.3 [11]. On the other hand, the measured width at $\sqrt{s_{NN}} = 200$ at RHIC is ≈ 2 for pions [12], and the antiparticle/particle ratio is apparently stable over a rapidity window of about 2 units around midrapidity [13]. These two observations indicate that extracting the characteristics of the average source at midrapidity by using midrapidity ratios is indeed possible at center-of-mass energies $\mathcal{O}(100)$ GeV. Then, we conclude that the use of full phase space multiplicities is better suited over the energy ranges of AGS and SPS, which we are examining in the present work, whereas midrapidity particle ratios can be used at RHIC energies to determine the characteristics of the central source. Even though a statistical model fit to full phase space multiplicities at RHIC in principle may be attempted, provided that the EGC condition applies, the presently available data set is not sufficient to make a reliable assessment.

III. THE DATA ANALYSIS

The experimental data set consists of measurements performed by the NA49 Collaboration in p - p (all inelastic reactions), C-C (15.3% most central), and Si-Si (12.2% most central) collisions at beam momentum of 158A GeV as well as Pb-Pb collisions at beam momenta of 20A, 30A, 40A, 80A, and 158A GeV (corresponding to $\sqrt{s_{NN}} = 6.2, 7.5, 8.7, 12.3,$ and 17.2 GeV, respectively). The Pb-Pb data set corresponds to 7% most central events except at top energy, where only 5% was selected. We also refit measurements in Au-Au collisions at 11.6A GeV of beam momentum (corresponding to $\sqrt{s_{NN}} = 4.7$ GeV) by using the new hadronic data set input [14].

The analysis is performed by searching the minima of the χ^2 , that is,

$$\chi^2 = \sum_i \frac{(N_i^{\text{exp}} - N_i^{\text{theo}})^2}{\sigma_i^2}, \quad (7)$$

in which N_i is the full phase space of the i th hadron species and $\sigma_i = \sqrt{(\sigma_i^{\text{stat}})^2 + (\sigma_i^{\text{sys}})^2}$ is the sum in quadrature of statistical and systematic experimental error.

The theoretical multiplicities are calculated by adding the primary multiplicities to the contribution from secondary decays. In order to make a proper comparison with the data, the decay chain is stopped so as to match the experimental definition of a measured particle. For SPS data, weakly decaying particles are considered as stable, except Λ and $\bar{\Lambda}$ at 20A and 30A GeV; whereas for AGS Au-Au collisions,

weak decays of hyperons and K_S^0 are performed. The final experimental and theoretical multiplicities used in our analysis are shown in Tables I–III.

We performed the analysis with two independent programs, hereafter referred to as analyses A and B, to cross-check the results and to assess the stability of the fits. We found only small discrepancies between the different analyses, mainly owing to a different method of treating hidden strangeness, branching ratios, and a slightly different particle input. The effect of uncertainties in masses, widths, and branching ratios have been shown to be negligible [7], and the difference in results between the two analyses arises solely from the different selection of the included hadronic states. The observed differences in the fit parameters between A and B are of the order of the fit errors, and they may be considered as an estimate of the systematic error due to uncertainties in the implementation of the model.

We give two different errors for the fitted parameters and derived quantities in Table IV, the first being the error coming from the fitting program (inferred from the analysis of the $\chi^2 = \chi_{\text{min}}^2 + 1$ level contours), while the second one is the error rescaled by a factor $\sqrt{\chi_{\text{min}}^2/\text{dof}}$ where dof is the number of degrees of freedom. We deem that the latter is a more realistic uncertainty on the parameters because of the ‘‘imperfect’’ $\chi_{\text{min}}^2/\text{dof}$ values (for further details, see Refs. [7, 14]), and thus the rescaled errors are used in all plots in this paper.

A. Main version

In our main version of the model, we fit the parameters T , V , μ_B and the strangeness under-saturation parameter γ_S ; for the relevant formulas, see Ref. [7]. This version of the model is called SHM(γ_S). We note that in the SHM(γ_S), the system volume V coincides with the so-called strangeness correlation volume [32]; the case of a nontrivial strangeness correlation volume has been studied by some of us in Ref. [7]. The resulting SHM(γ_S) parameters (see Table IV and Figs. 1–4) are smoothly varying functions of the beam energy, and no signs of anomalies are present. The fits have been performed in the supposedly sufficient statistical ensemble, i.e., canonical (exact conservation of strangeness, electric charge, and baryon number) for p - p collisions, S canonical (exact conservation of strangeness, but with grand-canonical treatment of electric charge and baryon number) in C-C and Si-Si collisions, and grand canonical (GC) for Pb-Pb collisions.

Indeed, for C-C collisions, where the number of participants is quite small, we cross-checked our main S -canonical calculation with a full canonical calculation in which the baryon number has been set to the nearest integer to the measured average number of participants. Very little deviation has been found between the two schemes for all particles, thus confirming the fitness of the S -canonical ensemble. On the other hand, the grand-canonical ensemble is not well suited for either C-C or Si-Si collisions. By using the best fit parameters in the two pictures and comparing the fitted yields, we found that for these systems, the GC ensemble overestimates the yield of multiply strange hyperons like Ω^- by 32% and 14%, respectively, with respect to the S -canonical

TABLE I. Comparison between measured and fitted particle multiplicities, in the framework of SHM(γ_S) model, in p - p and central C-C (15.3% most central) and Si-Si (12.2%) collisions at a beam energy of 158A GeV.

	p - p (canonical)			C-C S -canonical			Si-Si S -canonical		
	Measurement ^a	Fit A	Fit B	Measurement	Fit A	Fit B	Measurement	Fit A	Fit B
N_P				16.3 ± 1 [8]	15.79	15.98	41.4 ± 2 [8]	39.87	40.30
π^+	3.15 ± 0.16	3.25	3.28	22.4 ± 1.6 [8]	22.3	22.0	56.6 ± 4.1 [8]	57.4	56.47
π^-	2.45 ± 0.12	2.43	2.45	22.2 ± 1.6 [8]	22.3	22.0	57.6 ± 4.1 [8]	57.5	56.53
K^+	0.21 ± 0.02	0.228	0.200	2.54 ± 0.25 [8]	2.71	2.79	7.44 ± 0.74 [8]	7.99	8.17
K^-	0.13 ± 0.013	0.119	0.107	1.49 ± 0.16 [8]	1.46	1.51	4.42 ± 0.44 [8]	4.32	4.49
ϕ	0.012 ± 0.0015	0.0203 ^b	0.0149	0.18 ± 0.02 [8]	0.15	0.16	0.66 ± 0.09 [8]	0.48	0.51
Λ	0.115 ± 0.012	0.133	0.117	1.32 ± 0.32 [8]	1.62	1.69	3.88 ± 0.58 [8]	4.57	4.87
$\bar{\Lambda}$	0.0148 ± 0.0019	0.0147	0.0141	0.177 ± 0.028 [16]	0.149	0.182	0.492 ± 0.108 [16]	0.389	0.508
Ξ^-	0.0031 ± 0.0003	0.00285	0.00110 ^b		0.0728	0.0666		0.257	0.244
$\bar{\Xi}^+$	$9.2 \cdot 10^{-4} \pm 0.9 \cdot 10^{-5}$	0.000918	0.000388 ^b		0.0151	0.0161		0.0485	0.0562
Ω	$2.6 \cdot 10^{-4} \pm 1.3 \cdot 10^{-4}$	$8.87 \cdot 10^{-5}$	$2.12 \cdot 10^{-5}$ ^b		0.00397	0.00405		0.0181	0.0196
$\bar{\Omega}$	$1.6 \cdot 10^{-4} \pm 0.9 \cdot 10^{-4}$	$6.16 \cdot 10^{-5}$	$1.30 \cdot 10^{-5}$ ^b		0.00179	0.00216		0.00736	0.00979
p		1.094	1.125		7.01	7.18		17.2	17.6
\bar{p}	0.040 ± 0.007	0.0364	0.0445		0.303	0.367		0.714	0.879
K_S^0	0.18 ± 0.04	0.14	0.15		2.05	2.14		6.06	6.37
π^0		3.32	3.10		25.0	23.2		64.3	59.7
η		0.382	0.279		2.64	2.09		6.78	5.59
ω		0.342	0.299		2.33	2.00		5.85	5.04
η'		0.0328	0.0165		0.210	0.132		0.537	0.374
ρ^+		0.449	0.467		2.75	2.84		6.92	7.11
ρ^-		0.301	0.305		2.75	2.85		6.94	7.16
ρ^0		0.408	0.428		2.84	2.94		7.14	7.39
K^{*+}		0.0878	0.0673		0.978	0.933		2.80	2.72
K^{*-}		0.0359	0.0275		0.462	0.437		1.35	1.29
K^{*0}		0.0741	0.0563		0.964	0.926		2.76	2.70
\bar{K}^{*0}		0.0405	0.0316		0.455	0.431		1.33	1.27
Δ^{++}		0.281	0.263		1.62	1.52		3.92	3.69
$\bar{\Delta}^{--}$		0.0063	0.00701		0.0686	0.0748		0.160	0.177
Σ^+		0.0413	0.0321		0.444	0.429		1.26	1.24
Σ^-		0.0276	0.0213		0.435	0.421		1.23	1.21
Σ^0		0.0358	0.0276		0.440	0.424		1.25	1.22
$\bar{\Sigma}^-$		0.00339	0.00295		0.0413	0.0472		0.111	0.131
$\bar{\Sigma}^+$		0.00445	0.00388		0.0403	0.0461		0.107	0.128
$\bar{\Sigma}^0$		0.00407	0.00352		0.0409	0.0466		0.109	0.130
Ξ^0		0.00323	0.00126		0.0740	0.0676		0.262	0.248
$\bar{\Xi}^0$		0.000849	0.000351		0.0152	0.0164		0.0494	0.0572
$\Lambda(1520)$	0.012 ± 0.003	0.0106	0.00787		0.116	0.110		0.321	0.313

^aAll data in this column are from Ref. [15].

^bExcluded from the data sample in the fit.

ensemble. This clearly indicates that the S -canonical scheme is necessary.

The quality of the fits can be regarded as satisfactory overall, although not really good from a statistical point of view (except in Au-Au and C-C collisions) as χ^2/dof are generally of the order of 2–3. The worst fits are in Pb-Pb collisions at 20A and 30A GeV, with $\chi^2/\text{dof} \sim 3$ –4; this is because of specific deviations involving strange particles, which will be discussed in detail later in Sec. V.

A special mention is needed for p - p collisions. As has been mentioned, theoretical multiplicities have been calculated in the canonical ensemble, which is described in detail in

Ref. [16]. As far as strangeness under-saturation is concerned, in analysis B, the usual parametrization with γ_S was used. On the other hand, in analysis A, a parametrization described in Ref. [33] was used in which it is assumed that some number of $s\bar{s}$ pairs, in a Poisson distribution, hadronize. The parameter γ_S is thus replaced by the mean number $\langle s\bar{s} \rangle$ of these $s\bar{s}$ pairs. In general, for p - p , it was not possible to achieve a satisfactory fit in both models. We believe that this owes to the inadequacy of the canonical ensemble at this relatively low energy, where microcanonical effects play a nonnegligible role [17]. For analysis A, a good fit was obtained by removing the ϕ meson from the data sample, whose predicted yield deviated from

TABLE II. Comparison between measured and fitted particle multiplicities, in the framework of SHM(γ_S) model, in central Au-Au collisions (3%) at 11.6A GeV as well as Pb-Pb collisions (7%) at beam energies of 20A and 30A GeV.

	Au-Au 11.6A GeV (GC ensemble)			Pb-Pb 20A GeV (GC ensemble)			Pb-Pb 30A GeV (GC ensemble)		
	Measurement	Fit A	Fit B	Measurement	Fit A	Fit B	Measurement	Fit A	Fit B
N_p	363 ± 10 [17]	365.6	360.6	$349 \pm 1 \pm 5$ [6]	347.5	347.3	$349 \pm 1 \pm 5$ [18]	350.2	350.2
π^+	133.7 ± 9.93 [19, 20]	135.7	129.4	$184.5 \pm 0.6 \pm 13$ [6]	193.7	193.3	$239 \pm 0.7 \pm 17$ [18]	247.5	254.3
π^-		177.7	156.1	$217.5 \pm 0.6 \pm 15$ [6]	221.4	220.7	$275 \pm 0.7 \pm 19$ [18]	276.2	283.2
K^+	23.7 ± 2.86 [17]	18.7	18.8	$40.0 \pm 0.8 \pm 2.0$ [6]	34.4	35.7	$55.3 \pm 1.6 \pm 2.8$ [18]	44.8	43.9
K^-	3.76 ± 0.47 [17]	3.90	3.54	$10.4 \pm 0.12 \pm 0.5$ [6]	10.5	10.4	$16.1 \pm 0.2 \pm 0.8$ [18]	16.3	16.1
ϕ		0.327	0.350	1.91 ± 0.45 [6]	1.20	1.44	1.65 ± 0.17 [18]	2.01	2.08
Λ	18.1 ± 1.9 [7, 21, 22]	19.7	19.6	28.0 ± 1.5 [23]	28.8	31.2	$41.9 \pm 2.1 \pm 4.0$ [23]	33.8	34.5
$\bar{\Lambda}$	0.017 ± 0.005 [7, 21, 22]	0.017	0.011	0.16 ± 0.03 [24]	0.11	0.16	0.50 ± 0.04 [23]	0.35	0.49
p/π^+	1.23 ± 0.13 [20, 25]	1.27	1.22						
Ξ^-		0.551	0.557		1.37	1.42		1.85	1.66
Ξ^+		0.00221	0.00244		0.0215	0.0340		0.0645	0.0846
Ω		0.0132	0.0147		0.0618	0.0758		0.105	0.104
$\bar{\Omega}$		0.000367	0.000571		0.00436	0.00936		0.0134	0.0204
p		172.5	155.1		143.6	142.0		142.0	142.6
\bar{p}		0.0302	0.0124		0.144	0.170		0.467	0.625
K_S^0		11.6	11.7		22.7	23.8		30.7	30.6
π^0		164.5	146.7		224.2	215.3		286.2	280.8
η		8.17	6.83		16.7	15.2		24.5	21.8
ω		5.03	3.62		11.3	9.50		17.8	15.9
η'		0.335	0.243		0.938	0.818		1.58	1.30
ρ^+		7.74	10.3		15.2	18.5		22.5	26.7
ρ^-		9.19	12.6		17.5	21.5		25.5	30.4
ρ^0		8.56	11.5		16.6	20.4		24.6	29.2
K^{*+}		3.59	3.50		8.38	8.93		12.4	12.2
K^{*-}		0.627	0.513		2.19	2.07		3.93	3.67
K^{*0}		3.80	3.81		8.75	9.50		12.9	12.8
\bar{K}^{*0}		0.564	0.459		2.01	1.89		3.65	3.41
Δ^{++}		25.6	24.2		26.5	25.4		27.9	26.8
$\bar{\Delta}^-$		0.00330	0.00222		0.0296	0.0332		0.100	0.126
Σ^+		4.81	4.75		7.54	7.65		8.92	8.46
Σ^-		5.43	5.48		8.30	8.49		9.67	9.21
Σ^0		5.13	5.10		7.94	8.05		9.32	8.82
$\bar{\Sigma}^-$		0.00363	0.00323		0.0329	0.0449		0.103	0.136
$\bar{\Sigma}^+$		0.00295	0.00257		0.0278	0.0379		0.0889	0.118
$\bar{\Sigma}^0$		0.00328	0.00288		0.0303	0.0412		0.0959	0.127
Ξ^0		0.537	0.535		1.34	1.39		1.83	1.62
$\bar{\Xi}^0$		0.00248	0.00270		0.0231	0.0366		0.0686	0.0899
$\Lambda(1520)$		0.776	0.777		1.47	1.58		1.94	1.91

the data around 70%; indeed, the inclusion of ϕ leads the fit toward exceedingly high temperatures. For analysis B, a fair fit was obtained by removing the Ξ and Ω baryons from the data sample. Also in this case, the discrepancy between central data value and the model is considerable, but it should be also noted that the likely microcanonical effects are the largest for heavy baryons in p - p collisions [34]. In general, it seems that the parametrization with $\langle s\bar{s} \rangle$ leads to a better agreement with the data in comparison with the γ_S parametrization, according to a cross-test performed in the framework of analysis A.

B. Proper volume

We have amended our fits by implementing extended hadrons instead of pointlike particles. Our calculations follow the model in Ref. [35], with a primary average multiplicity of

the species j in the grand-canonical ensemble reading, in the limit of Boltzmann statistics,

$$\langle n_j \rangle = \frac{\langle n_j \rangle_{\text{pl}} e^{-v_j \xi}}{1 + \sum_k \langle n_k \rangle_{\text{pl}} e^{-v_k \xi}}, \quad (8)$$

where $\langle n_j \rangle_{\text{pl}}$ is the hadron multiplicity in the pointlike case, ξ is the solution of the equation

$$\xi = \sum_k \frac{\langle n_k \rangle_{\text{pl}}}{V} e^{-v_k \xi}, \quad (9)$$

and v_j is the proper volume, or eigenvolume, of the hadron. This volume effectively introduces a repulsive hard-core interaction in the hadron gas equation of state, yet it is an unknown quantity, and one has to make some assumptions to develop calculations. If it was the same for all hadrons, there would be no corrections to the intensive parameters, as the ratio between different species would be the same [this

TABLE III. Comparison between measured and fitted particle multiplicities, in the framework of SHM(γ_S) model, in central Pb-Pb collisions at beam energies of 40 and 80 (7% most central) and 158A GeV (5% most central). The measured $\Lambda(1520)$ yield has been removed from the fitted data sample at 158A GeV.

	Pb-Pb 40A GeV (GC ensemble)			Pb-Pb 80A GeV (GC ensemble)			Pb-Pb 158A GeV (GC ensemble)		
	Measurement	Fit A	Fit B	Measurement	Fit A	Fit B	Measurement	Fit A	Fit B
N_p	$349 \pm 1 \pm 5$ [26]	351.4	351.2	$349 \pm 1 \pm 5$ [26]	351.2	351.0	$362 \pm 1 \pm 5$ [26]	363.2	363.4
π^+	$293 \pm 3 \pm 15$ [26]	283.4	285.1	$446 \pm 5 \pm 22$ [26]	420.1	419.4	$619 \pm 17 \pm 31$ [26]	550.0	533.6
π^-	$322 \pm 3 \pm 16$ [26]	312.6	314.6	$474 \pm 5 \pm 23$ [26]	450.6	450.4	$639 \pm 17 \pm 31$ [26]	582.0	565.9
K^+	$59.1 \pm 1.9 \pm 3$ [26]	52.1	52.1	$76.9 \pm 2 \pm 4$ [26]	71.6	71.0	$103 \pm 5 \pm 5$ [26]	103.1	103.6
K^-	$19.2 \pm 0.5 \pm 1.0$ [26]	20.8	20.8	$32.4 \pm 0.6 \pm 1.6$ [26]	36.5	36.4	$51.9 \pm 1.9 \pm 3$ [26]	59.3	59.3
ϕ	2.50 ± 0.25 [6]	2.70	2.77	4.58 ± 0.20 [6]	4.43	4.46	7.6 ± 1.1 [26]	8.01	8.59
Λ	$43.0 \pm 1.9 \pm 3.4$ [27]	37.1	38.2	$44.7 \pm 2.8 \pm 3.2$ [27]	42.4	43.2	$44.9 \pm 3.5 \pm 5.4$ [27]	53.6	55.9
$\bar{\Lambda}$	$0.66 \pm 0.04 \pm 0.06$ [27]	0.67	0.64	$2.02 \pm 0.25 \pm 0.20$ [27]	2.16	2.11	$3.74 \pm 0.19 \pm 0.43$ [27]	4.83	4.96
Ξ^-	$2.41 \pm 0.15 \pm 0.24$ [28]	2.20	2.10		2.83	2.62	4.45 ± 0.22 [26]	4.42	4.31
$\bar{\Xi}^+$		0.122	0.112		0.330	0.298	0.83 ± 0.04 [26]	0.79	0.78
Ω		0.143	0.148		0.222	0.221	$0.59 \pm 0.12 \pm 0.04$ [29]	0.44	0.49
$\bar{\Omega}$		0.0262	0.0268		0.0623	0.0610	$0.26 \pm 0.06 \pm 0.03$ [29]	0.16	0.19
$\Omega + \bar{\Omega}$	$0.14 \pm 0.03 \pm 0.04$ [29]	0.17	0.18						
p		140.8	140.7		140.8	141.3		143.4	142.8
\bar{p}		0.897	0.821		3.32	3.21		6.86	6.70
K_S^0		36.4	37.1		53.5	54.4	81 ± 4 [30]	80.0	82.6
π^0		328.1	314.1		485.0	458.1		636.2	581.6
η		30.2	26.1		49.5	41.6		70.5	62.2
ω		22.7	18.5		39.9	33.0		55.4	44.7
η'		2.11	1.60		3.76	2.75		5.73	4.41
ρ^+		27.9	29.7		46.7	47.2		63.4	60.9
ρ^-		31.3	33.5		50.9	51.8		68.2	66.1
ρ^0		30.3	32.5		50.2	51.1		68.0	66.1
K^{*+}		15.6	14.3		23.0	20.9		34.2	31.8
K^{*-}		5.41	4.80		10.6	9.46		18.0	16.2
K^{*0}		15.6	14.9		23.5	21.6		34.7	32.5
\bar{K}^{*0}		5.06	4.47		10.0	8.95		17.2	15.5
Δ^{++}		28.7	26.4		29.9	27.5		30.9	28.1
$\bar{\Delta}^-$		0.198	0.163		0.747	0.650		1.55	1.36
Σ^+		9.79	9.47		11.3	10.8		14.4	14.0
Σ^-		10.5	10.2		11.9	11.4		15.0	14.6
Σ^0		10.2	9.83		11.6	11.1		14.7	14.3
$\bar{\Sigma}^-$		0.197	0.179		0.623	0.577		1.38	1.34
$\bar{\Sigma}^+$		0.172	0.157		0.561	0.520		1.26	1.23
$\bar{\Sigma}^0$		0.185	0.167		0.592	0.547		1.32	1.28
Ξ^0		2.17	2.07		2.81	2.60		4.41	4.29
$\bar{\Xi}^0$		0.129	0.119		0.345	0.312		0.823	0.812
$\Lambda(1520)$		2.27	2.09		2.78	2.53	1.57 ± 0.44 [31]	3.64	3.41

can be seen from Eq. (8)]. We tested the assumption of an eigenvolume v_j proportional to the mass through a baglike constant B . In this case, one expects an upward shift in the temperature $\Delta T \simeq T^2 B \xi$, since for masses $m \gg T$, one has

$$\langle n_j \rangle \propto \left(\frac{mT}{2\pi} \right)^{3/2} e^{-m_j/T - B\xi m_j}, \quad (10)$$

with all other fit parameters almost unchanged. Indeed, we found that for several reasonable values of the constant B , from 0.5 to 2 fm³/GeV, the only effect in the fit was a temperature rise by the expected amount without any decrease in the χ^2 , that is in the fit quality. We therefore conclude that the introduction of this effect, at least in the model of Ref. [35], does not entail an improvement of the data-model agreement with respect to the pointlike picture.

C. Two-component model

In this picture, henceforth referred to as SHM(TC), the observed hadron production is assumed to stem from the superposition of two components (TC): One originated from one or more fireballs in full chemical equilibrium and another component from peripheral single nucleon-nucleon collisions where final particles escape the interaction region. The idea of this model is to ascribe the observed under-saturation of strangeness in heavy ion collisions to the N - N component, leaving the large fireballs at complete equilibrium, i.e., with $\gamma_S = 1$. Of course, this is possible provided that the mean number of single nucleon-nucleon collisions $\langle N_c \rangle$ is sufficiently large. We note that similar approaches have been proposed in the literature, in which the role of the second component besides the main fireball is played by a smaller peripheral fireball with different thermodynamic parameters

TABLE IV. Summary of fitted parameters in nuclear collisions at AGS and SPS energies in the framework of the SHM(γ_S) model. Also quoted are the strangeness chemical potential, minimum χ^2 estimated radius of the EGC, and λ_S parameter (see Sec. III). The rescaled errors (see text) are quoted within parentheses. For p - p at 158A GeV of beam energy, we have fitted mean number of $s\bar{s}$ pairs (analysis A) and fitted γ_S (analysis B).

Parameters	Main analysis A	Main analysis B	Main analysis A	Main analysis B
	p - p 158A GeV (C ensemble)		Au-Au 11.6A GeV (GC ensemble)	
T (MeV)	181.5 ± 3.4^a	$178.2 \pm 4.8(5.9)$	$118.7 \pm 2.7(3.1)$	$119.2 \pm 3.9(5.3)$
μ_B (MeV)			$554.4 \pm 11.3(13.0)$	$578.8 \pm 15.4(20.9)$
γ_S	$0.461 \pm 0.020^{a,b}$	$0.446 \pm 0.018(0.023)$	$0.640 \pm 0.060(0.069)$	$0.768 \pm 0.086(0.116)$
$VT^3 \exp[-0.7 \text{ GeV}/T]$	$6.2 \pm 0.5^{a,c}$	$0.127 \pm 0.005(0.006)$	$1.99 \pm 0.17(0.20)$	$1.47 \pm 0.18(0.25)$
χ^2/dof	$8.4/10^a$	$10.8/7$	$4.0/3$	$5.5/3$
R (fm)		$1.28 \pm 0.08(0.10)$	$9.25 \pm 0.60(0.69)$	$8.28 \pm 0.71(0.96)$
λ_S	0.266 ± 0.019	$0.195 \pm 0.005(0.006)$	$0.380 \pm 0.050(0.058)$	$0.489 \pm 0.083(0.11)$
	C-C 158A GeV (S -canonical ensemble)		Si-Si 158A GeV (S -canonical ensemble)	
T (MeV)	$166.0 \pm 4.4(4.4)$	166.1 ± 4.2	$162.2 \pm 4.9(7.9)$	$163.3 \pm 3.0(4.1)$
μ_B (MeV)	$262.6 \pm 12.8(12.9)$	249.0 ± 12.6	$260.0 \pm 11.1(17.9)$	$246.4 \pm 11.0(15.1)$
γ_S	$0.547 \pm 0.041(0.041)$	0.578 ± 0.043	$0.621 \pm 0.047(0.076)$	$0.668 \pm 0.049(0.067)$
$VT^3 \exp[-0.7 \text{ GeV}/T]$	$0.89 \pm 0.06(0.06)$	0.83 ± 0.05	$2.22 \pm 0.14(0.22)$	$2.07 \pm 0.13(0.18)$
χ^2/dof	$4.1/4$	$3.4/4$	$10.4/4$	$7.6/4$
R (fm)	$2.89 \pm 0.19(0.19)$	2.82 ± 0.19	$4.15 \pm 0.30(0.48)$	$3.99 \pm 0.19(0.27)$
λ_S	$0.373 \pm 0.031(0.032)$	0.364 ± 0.034	$0.414 \pm 0.033(0.054)$	$0.418 \pm 0.036(0.049)$
	Pb-Pb 20A GeV (GC ensemble)		Pb-Pb 30A GeV (GC ensemble)	
T (MeV)	$131.3 \pm 2.3(4.5)$	$135.8 \pm 3.2(5.2)$	$140.1 \pm 1.6(3.3)$	$144.3 \pm 1.9(4.7)$
μ_B (MeV)	$466.7 \pm 6.5(12.9)$	$472.5 \pm 8.6(13.7)$	$413.7 \pm 8.0(16.3)$	$406.0 \pm 8.0(19.1)$
γ_S	$0.773 \pm 0.037(0.072)$	$0.885 \pm 0.053(0.086)$	$0.773 \pm 0.041(0.084)$	$0.798 \pm 0.040(0.099)$
$VT^3 \exp[-0.7 \text{ GeV}/T]$	$4.41 \pm 0.23(0.45)$	$3.88 \pm 0.26(0.42)$	$6.91 \pm 0.40(0.80)$	$6.52 \pm 0.35(0.84)$
μ_S (MeV)	101.2	114.2	93.2	99.8
χ^2/dof	$15.5/4$	$10.3/4$	$16.5/4$	$23.0/4$
R (fm)	$9.05 \pm 0.41(0.80)$	$7.89 \pm 0.46(0.73)$	$8.80 \pm 0.32(0.64)$	$7.99 \pm 0.33(0.79)$
λ_S	$0.477 \pm 0.035(0.069)$	$0.586 \pm 0.056(0.089)$	$0.500 \pm 0.037(0.073)$	$0.517 \pm 0.039(0.093)$
	Pb-Pb 40A GeV (GC ensemble)		Pb-Pb 80A GeV (GC ensemble)	
T (MeV)	$146.1 \pm 2.2(3.0)$	$143.0 \pm 2.3(3.1)$	$153.5 \pm 2.5(4.1)$	$149.9 \pm 3.2(5.1)$
μ_B (MeV)	$382.4 \pm 6.8(9.1)$	$380.8 \pm 6.6(8.9)$	$298.2 \pm 5.9(9.6)$	$293.8 \pm 6.9(11.0)$
γ_S	$0.779 \pm 0.033(0.045)$	$0.857 \pm 0.037(0.050)$	$0.740 \pm 0.024(0.040)$	$0.797 \pm 0.031(0.049)$
$VT^3 \exp[-0.7 \text{ GeV}/T]$	$8.75 \pm 0.40(0.54)$	$7.57 \pm 0.35(0.48)$	$15.25 \pm 0.61(0.99)$	$13.53 \pm 0.64(1.03)$
μ_S (MeV)	89.5	89.5	69.6	68.4
χ^2/dof	$10.9/6$	$11.0/6$	$10.6/4$	$10.2/4$
R (fm)	$8.53 \pm 0.35(0.47)$	$8.59 \pm 0.35(0.48)$	$9.05 \pm 0.38(0.62)$	$9.23 \pm 0.44(0.70)$
λ_S	$0.523 \pm 0.032(0.043)$	$0.513 \pm 0.031(0.042)$	$0.474 \pm 0.023(0.038)$	$0.443 \pm 0.021(0.034)$
	Pb-Pb 158A GeV (GC ensemble)			
T (MeV)	$157.5 \pm 1.6(2.5)$	$154.6 \pm 1.5(2.7)$		
μ_B (MeV)	$248.9 \pm 5.7(9.0)$	$245.9 \pm 5.6(10.0)$		
γ_S	$0.842 \pm 0.027(0.042)$	$0.941 \pm 0.030(0.054)$		
$VT^3 \exp[-0.7 \text{ GeV}/T]$	$20.91 \pm 0.87(1.39)$	$18.21 \pm 0.75(1.35)$		
μ_S (MeV)	59.3	59.5		
χ^2/dof	$22.5/9$	$29.1/9$		
R (fm)	$9.42 \pm 0.27(0.44)$	$9.42 \pm 0.27(0.48)$		
λ_S	$0.526 \pm 0.020(0.032)$	$0.508 \pm 0.020(0.036)$		

^aIn fit A of p - p collisions, the ϕ meson has been excluded from the data sample because it biased the fit toward an exceedingly high temperature. Final χ^2 does not then take into account the large deviation of ϕ meson yield.

^bIn fit A of p - p collisions, the γ_S parameter is to be replaced by the mean number $\langle s\bar{s} \rangle$ of strange quark pairs.

^cIn fit A of p - p collisions, the parameter $VT^3 \exp[-0.7 \text{ GeV}/T]$ is to be replaced by VT^3 .

or by a collection of clusters [36]. It should be mentioned that the SHM(TC) picture is quite a simplified one: it is assumed that particles emerging from N - N collisions decouple without further reinteraction, whereas collisions in the core of the system eventually lead to a hadron gas in perfect equilibrium. These are sharp approximations that would certainly need a refinement in more accurate studies.

In the SHM(TC) model, then, the overall hadron multiplicity can be written as

$$\langle n_j \rangle = \langle N_c \rangle \langle n_j \rangle_{NN} + \langle n_j \rangle_V, \quad (11)$$

where $\langle n_j \rangle_{NN}$ is the average multiplicity of the j th hadron in a single N - N collision and $\langle n_j \rangle_V$ is the average multiplicity of hadrons emitted from the equilibrated fireball with $\gamma_S = 1$.

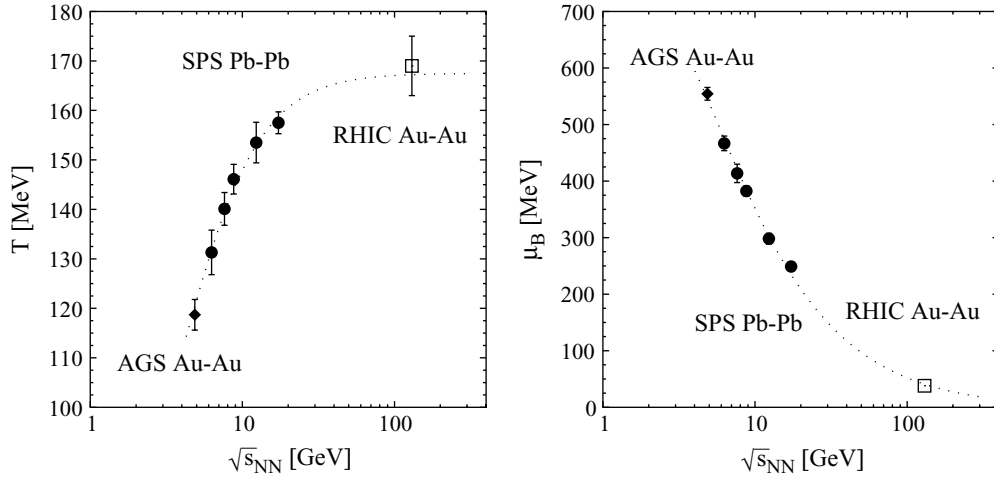


FIG. 1. Fitted temperatures and baryon chemical potentials at chemical freeze-out (analysis A) as a function of the N - N center-of-mass energy in central heavy ion collisions. Dashed lines were evaluated with the Eqs. (15) and (17). The RHIC point obtained with a fit to hadron ratios at midrapidity [43], is the open square.

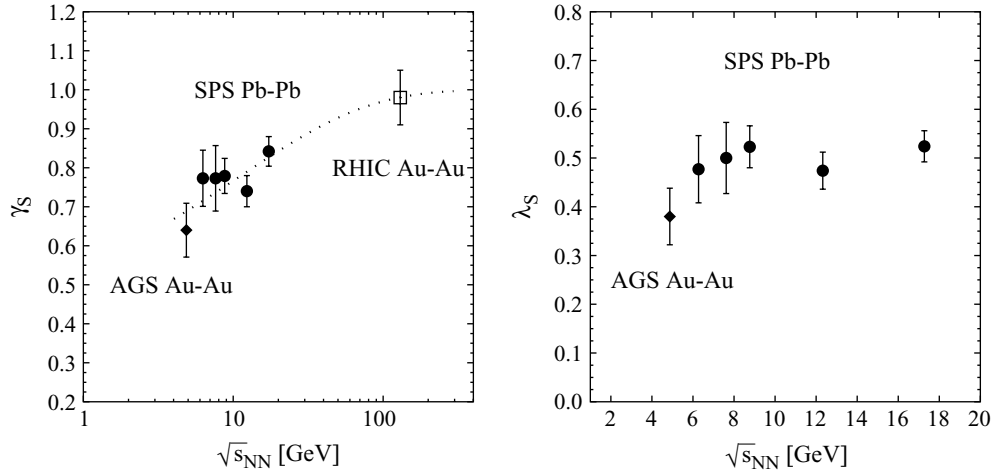


FIG. 2. Strangeness under-saturation parameter γ_S and Wroblewski factor λ_S at chemical freeze-out (analysis A) as a function of N - N center-of-mass energy in central heavy ion collisions. Dashed line was evaluated with Eq. (20). The RHIC point, obtained with a fit to hadron ratios at midrapidity [43] is the open square.

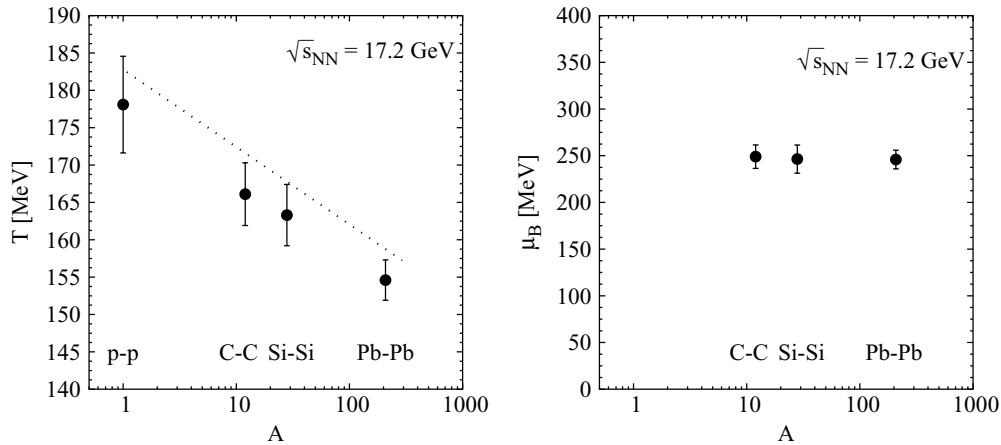


FIG. 3. Fitted temperature and baryon chemical potential at chemical freeze-out as a function of A in central heavy ion collisions at $\sqrt{s_{NN}} = 17.2$ GeV. From left to right: p - p , C-C, Si-Si, and Pb-Pb points fitted in analysis B. Dashed line was evaluated with Eq. (19), which has been fitted to the points of analysis A. The observed systematic shift between data and interpolation is mainly a reflection of the slight difference ($\simeq 3$ – 4 MeV) between temperature in analyses A and B in Pb-Pb and p - p .

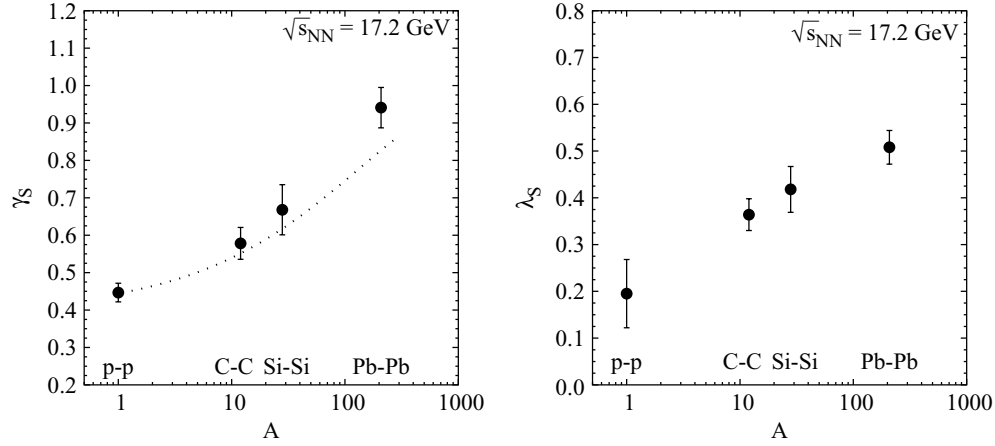


FIG. 4. Strangeness suppression factor γ_S and Wroblewski factor λ_S at chemical freeze-out as a function of A in central heavy ion collisions at $\sqrt{s_{NN}} = 17.2$ GeV (analysis B). Dashed line was evaluated with Eq. (20).

The $\langle n_j \rangle_{NN}$ term can be written in turn as

$$\langle n_j \rangle_{NN} = \frac{Z^2}{A^2} \langle n_j \rangle_{pp} + \frac{(A-Z)^2}{A^2} \langle n_j \rangle_{nn} + \frac{2Z(A-Z)}{A^2} \langle n_j \rangle_{np}. \quad (12)$$

To calculate $\langle n_j \rangle_{NN}$, we used the statistical model and fitted p - p full phase space multiplicities measured at the same beam energy by the same NA49 experiment (see Table I). For n - p and n - n collisions, the parameters of the statistical model determined in p - p are retained and the initial quantum numbers are changed accordingly.

We fitted T , V , and μ_B of the equilibrated fireballs and $\langle N_c \rangle$ by using NA49 data in C-C, Si-Si, and Pb-Pb collisions at 158A GeV in analysis A. It should be mentioned that in this fit, the systematic error on the refitted parameters caused by to the uncertainty on statistical model parameters in N - N collisions (i.e., the errors quoted in Table IV for p - p collisions), used as input, has been disregarded. The resulting fit parameters are

shown in Table V. For the Pb-Pb system, the fit quality, as well as the obtained values of T and μ_B , are comparable to the main fit within the SHM(γ_S) model. The predicted number of single N - N collisions is about 25. Thus, on average, only 310 nucleons out of 360 participants contribute to the formation of large equilibrated fireballs. In the case of Si-Si, the fit quality is significantly improved compared to the main version of the statistical model, and the resulting fit parameters are comparable to the ones in Table V. The number of independent N - N collisions is 12 ± 4 , suggesting that more than half of the 41 participating nucleons collide only once.

Being so small, the C-C system needs special treatment when the two-component model is applied. Since there are only 16 participants in the system, one has to calculate both components in full canonical ensemble. This means that one has to take explicitly into account all the different proton-neutron configurations in the central fireball and extract those nucleons participating in the fireball from the “nucleon pool” available for the single N - N collisions. It seems that even C-C

TABLE V. Fit results in central C-C, Si-Si, and Pb-Pb collisions at 158A GeV within the two-component model SHM(TC) and with $\langle N_c \rangle$ as free parameter (top section) as well as with $\langle N_c \rangle$ fixed to the value calculated in the Glauber model (bottom section). The rescaled errors (see text) are quoted within parentheses.

Parameters	C-C, canonical ensemble	Si-Si, S-canonical ensemble	Pb-Pb, GC ensemble
T (MeV)	$172.4 \pm 11.8(12.6)$	162.0 ± 7.6	$153.9 \pm 1.5(2.5)$
μ_B (MeV)		234.4 ± 22.5	$240.8 \pm 6.9(11.8)$
γ_S	1.0 (fixed)	1.0 (fixed)	1.0 (fixed)
$VT^3 \exp[-0.7 \text{ GeV}/T]$	$0.23 \pm 0.034(0.037)$	0.91 ± 0.11	$16.11 \pm 0.57(0.97)$
$\langle N_c \rangle$	$6.0 \pm 0.4(0.4)$	11.4 ± 1.8	$25 \pm 10(16)$
χ^2/dof	5.8/4	1.0/4	26.3/9
Parameters	C-C, S-canonical ensemble	Si-Si, S-canonical ensemble	Pb-Pb, GC ensemble
T (MeV)	$161.0 \pm 9.1(25.9)$	$151.1 \pm 7.1(16.4)$	$154.7 \pm 1.5(2.9)$
μ_B (MeV)	$315 \pm 18(50)$	$285 \pm 13(31)$	$261.6 \pm 2.6(4.6)$
γ_S	1.0 (fixed)	1.0 (fixed)	1.0 (fixed)
$VT^3 \exp[-0.7 \text{ GeV}/T]$	$0.31 \pm 0.028(0.071)$	$1.19 \pm 0.06(0.12)$	$16.54 \pm 0.44(0.84)$
$\langle N_c \rangle$	2.67 (fixed)	5.49 (fixed)	17.6 (fixed)
χ^2/dof	32/5	21.7/5	36.3/10

can be described with the two-component model if the baryon charge in the central fireball is ~ 4 . The resulting $\chi^2/\text{dof} \simeq 5.8/4$ with all the different n - p combinations in the completely equilibrated fireball, i.e., the fit quality is worse than with the main version of the statistical model, but the overall fit quality is still acceptable.

To cross-check these results, we calculated the number of single N - N collisions from the Glauber model and repeated the fits (in analysis B) the same way by fixing $\langle N_c \rangle$ as that coming from the Glauber calculations. We first implemented a Monte Carlo calculation of the Glauber model as follows:

- (i) At a given impact parameter, the number of collisions of each projectile nucleon is randomly extracted from a Poisson distribution whose mean is the product of the thickness function times the inelastic nucleon-nucleon cross section.
- (ii) Then, the number of collisions undergone by each nucleon belonging to the target nucleus is randomly extracted from a multinomial distribution constrained with the total number of collisions as determined in the previous step and whose weights are proportional to the product of their relevant thickness function times the inelastic nucleon-nucleon cross section.
- (iii) For each generated event, uniformly distributed in the transverse impact parameter plane, we keep track of the number of nucleons undergoing 0, 1, 2, . . . collisions N_0, N_1, N_2, \dots in both the projectile and the target nucleus.

The thickness function has been calculated on the basis of the Woods-Saxon distribution

$$\frac{dN}{dr} = \frac{n_0}{1 + e^{(r-R)/d}}. \quad (13)$$

with the parameters quoted in Ref. [37]: $n_0 = 0.17 \text{ fm}^{-3}$; $R = 1.12 - 0.86A^{-1/3} \text{ fm}$ and $d = 0.54 \text{ fm}$. For each event, this Monte Carlo calculation provides the number of nucleons $N_{1(a)}$ and $N_{1(b)}$ colliding once, in the projectile a and target nucleus b , respectively. In general, these two numbers differ because nucleons from a may collide once with a nucleon from b , which in turn collides with two or more nucleons from a . Therefore, the minimum between $N_{1(a)}$ and $N_{1(b)}$ is the maximal number of single nucleon-nucleon collisions per event, i.e.,

$$N_c \geq \min[N_{1(a)}, N_{1(b)}] \equiv N_m. \quad (14)$$

The equality sign applies only if the N_m nucleons from one nucleus collided with N_m nucleons of the other, all of them among those undergoing one collision. We assume this is always the case and hence take N_m as a fair estimate of the number of single collisions. The mean number of N_c is then averaged over the most central bin defined by the distribution of the number of projectile spectators according to the NA49 centrality selection method.

We determined the mean number of single N - N collisions within the most central bin to be 2.67, 5.49, and 17.6 for C-C, Si-Si, and Pb-Pb, respectively, at a beam energy of 158A GeV. By fixing N_c to the above numbers, we then fitted V , T , and μ_B of the equilibrated fireballs and found the results shown in

Table IV. The fit quality is sizably worse than in the previous case. Since the used number of collisions is actually an upper limit of single N - N collisions, we conclude that the SHM(TC) is disfavored by the data, if the Glauber model is assumed to be correct.

IV. ENERGY AND SYSTEM SIZE DEPENDENCE

We are now in a position to study the dependence of chemical freeze-out on beam energy and system size in central ultrarelativistic heavy ion collisions. According to what has been discussed at the end of Sec. II, for RHIC energy, we will include the parameters determined with fits to midrapidity particle multiplicity ratios.

The first observation is that the chemical freeze-out of different colliding systems at the same N - N center-of-mass energy, i.e., C-C, Si-Si, and Pb-Pb, seems to occur at similar values of the baryon chemical potential, namely, $\mu_B \approx 250 \text{ MeV}$ (see Fig. 3). Such weak system size dependence of the baryon chemical potential has already been reported [38]. On the other hand, systems with fewer participating nucleons seem to decouple at slightly higher temperatures than heavy systems (see Fig. 3). Nevertheless, generally speaking, the freeze-out condition seems to be determined mostly by the beam energy and little by the number of participants, also in peripheral collisions [38,39].

The dependence of the freeze-out parameters on the N - N center-of-mass energy in heavier systems (Pb-Pb and Au-Au) is shown in Figs. 1 and 2. The fitted points show a relatively strong dependence on energy, yet with a smooth behavior: Lower energies always correspond to a lower central temperature value and a higher baryon chemical potential.

A smooth dependence is also obtained for the chemical freeze-out in the μ_B - T plane, see Fig. 5; over the examined range of temperatures, all points lie, on a parabola corresponding to the chemical freeze-out condition $\langle E \rangle / \langle N \rangle \approx 1 \text{ GeV}$ [40]. Owing to the slight difference in temperature, the lighter systems C-C and Si-Si do not lie on the same curve, and this leads to the conclusion that at least in the model with γ_S only, the freeze-out curve depends on the colliding nucleus.

Conversely, the degree of chemical equilibration of strangeness seems to be strongly dependent on the number of participants and much less on the energy. This has been pointed out in several studies of peripheral Pb-Pb collision systems [38,39]. In fact, from small to large systems, γ_S increases monotonically from 0.45 in p - p to ~ 0.8 in Pb-Pb at the same beam energy, see Fig. 4, while the dependence on energy is much milder, with a variation from 0.65 to 0.84 over the 4.7–17.2 GeV energy range. Therefore, strangeness is not in chemical equilibrium up to the top SPS energy, and only for midrapidity yields at RHIC does γ_S seem to have attained 1 [41].

Strong suppression in strangeness production in small systems can be seen also in the Wroblewski variable $\lambda_S = 2\langle s\bar{s} \rangle / (\langle u\bar{u} \rangle + \langle d\bar{d} \rangle)$, the estimated ratio of newly produced strange quarks to u , d quarks at primary hadron level, shown in Figs. 2 and 4, and Table I. The calculation of newly produced quark pairs is performed by using the statistical model best-fit values of the various hadron multiplicities,

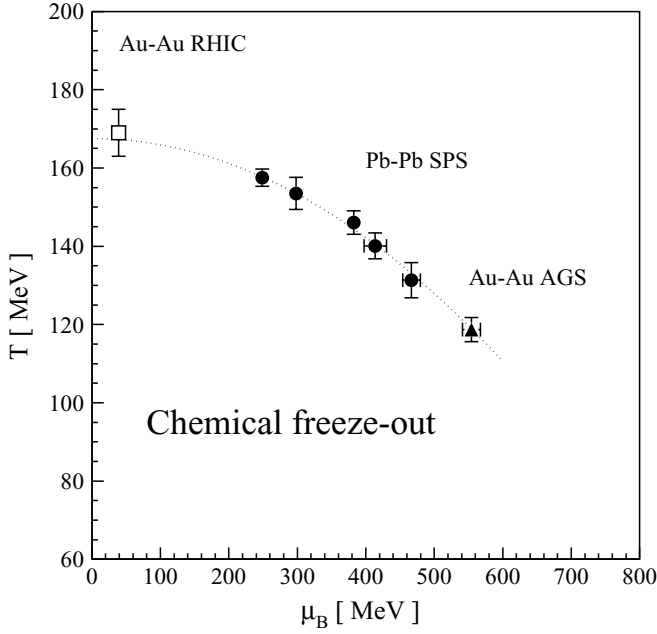


FIG. 5. Chemical freeze-out points in the μ_B - T plane for central Pb-Pb and Au-Au collisions. Dashed line shows the parabolic interpolation Eq. (15) obtained by fitting SPS and AGS points. The RHIC $\sqrt{s_{NN}} = 130$ GeV point, shown as an open square, was taken from Ref. [43].

so the obtained λ_S values are somehow model dependent. Nevertheless, this variable shows a very similar behavior as the γ_S parameter, indicating strong monotonic system size dependence in relative strangeness production.

It is also interesting to estimate the thermal energy content (defined as the internal energy $U = T^2 \partial \ln Z / \partial T|_{V, \mu/T}$, where Z is the grand-canonical partition function, hence including rest masses of hadrons and resonances plus their thermal kinetic energies) of the hadronic matter at freeze-out. Indeed, the fraction of thermal energy to the total available energy decreases rapidly as a function of energy, as shown in Fig. 6.

A. Interpolation of the statistical model parameters

It is worth trying to summarize the amount of information we have collected on the statistical model parameters at freeze-out in central collisions of different systems with some simple empirical interpolations. Some of them have already been proposed in previous works [7,42].

A satisfactory description of our Pb-Pb and Au-Au freeze-out points in the $T = \mu_B$ plane can be achieved by the simple parabolic fit

$$T \approx T_0 - b \mu_B^2, \quad T_0 = 167.5 \text{ MeV}, \quad b = 0.1583 \text{ GeV}^{-2}. \quad (15)$$

Note that the most recent determination [43] of T and μ_B in central Au-Au collisions at $\sqrt{s_{NN}} = 130$ GeV (169 ± 6 and 38 ± 5 MeV, respectively) also follows this dependence, see Fig. 5. Similarly, for γ_S , one can try to make an interpolation as a function of μ_B constrained by the requirement $\gamma_S \rightarrow 1$ when $\mu_B \rightarrow 0$, i.e., full chemical equilibrium at very large energy.

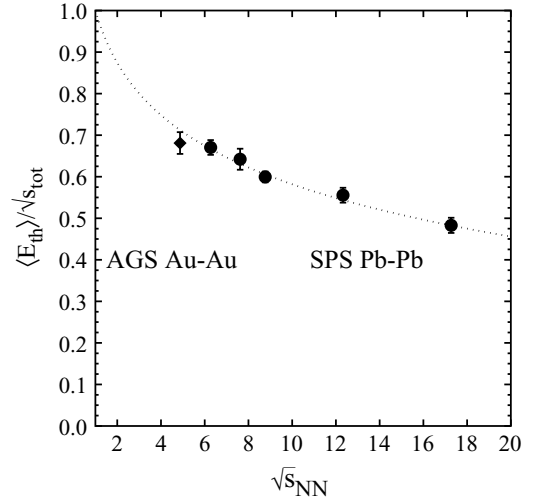


FIG. 6. Estimated fraction of the initial collision energy spent into thermal energy content in central heavy ion collisions as a function of the N - N center-of-mass energy. The line is of the form $f(\sqrt{s_{NN}}) = 1 - b \ln(\sqrt{s_{NN}})$ and fitted to all points.

The assumed functional form is then

$$\gamma_S = 1 - g \exp \left[-\frac{a}{\mu_B/T} \right], \quad (16)$$

and the resulting parameters are $g = 0.396$ and $a = 1.23$. Both fits to Eqs. (15) and (16) have $\chi^2/\text{dof} \approx 1$.

The next step is to provide an interpolation of μ_B as a function of $\sqrt{s_{NN}}$. Once this was known, it would be possible to predict the value of T and γ_S at any collision energy through the Eqs. (15) and (16). The main advantage of μ_B is that it is almost independent of the number of participants, so that a single function $\mu_B = \mu_B(\sqrt{s_{NN}})$ would apply to both light and heavy systems. We have interpolated μ_B with a function

$$\mu_B = \alpha \frac{\ln \sqrt{s_{NN}}}{(\sqrt{s_{NN}})^\beta}, \quad (17)$$

with $\alpha = 2.06$, $\beta = 1.13$, and energy is given in GeV. This interpolation gives a very good description of the energy dependence of the baryon chemical potential from $\sqrt{s_{NN}} = 4.7$ to 130 GeV.

We are now in a position to obtain the functions $T = T(\sqrt{s_{NN}}, A)$ and $\gamma_S = \gamma_S(\sqrt{s_{NN}}, A)$. According to Eqs. (15) and (17), we have

$$T = T_0 - C \left(\frac{\ln \sqrt{s_{NN}}}{(\sqrt{s_{NN}})^\beta} \right)^2, \quad (18)$$

where $C = b\alpha^2 \simeq 0.672$ and energy is given in GeV.

Furthermore, in order to take into account the dependence on system size, we introduce a very simple A dependence for the constant T_0 term. Looking at Fig. 3, one can easily realize that T_0 depends almost logarithmically on the mass number of the nucleus, thus it can be assumed $T_0 = T_c - \tau \ln A$ with $T_c \simeq 191.5$ MeV and $\tau \simeq 4.5$ MeV, leading to the final

expression of the chemical freeze-out temperature

$$T = 0.1915 - 0.0045 \ln A - 0.672 \left(\frac{\ln \sqrt{s_{NN}}}{(\sqrt{s_{NN}})^{1.13}} \right)^2, \quad (19)$$

where every quantity is expressed in GeV.

For γ_S , as its dependence on A is stronger than on $\sqrt{s_{NN}}$, it is more suitable to write down an independent interpolation formula rather than obtain one from Eqs. (15)–(17). By using

$$\gamma_S = 1 - \zeta \exp[-\xi \sqrt{A \sqrt{s_{NN}}}], \quad (20)$$

which is inspired by (17), a good fit is obtained by setting $\zeta = 0.606$ and $\xi = 0.0209$ (the energy is in GeV).

It should be finally emphasized that all of the above relations only apply to central collisions and cannot be used for peripheral nucleus-nucleus collisions. For instance, it has already been observed, indeed, that strangeness under-saturation scales not with the number of participants [38], but rather with the linear size of the fireballs [39].

V. DISCUSSION

In principle, by using Eqs. (15)–(20), it is possible to estimate, within the SHM, the average multiplicities and ratios of any particle species for any colliding system in central collisions at any energy. It is especially interesting to study possible deviations of some specific particle ratios from the predicted smooth dependence of our interpolations. Such deviations would be a signal that the SHM scheme has some problem and either some refinement is needed (e.g., the hypotheses underlying the global fit do not fully apply) or there is some specific mechanism beyond the statistical ansatz responsible for them.

Of special importance in this context is the anomalous peak (“horn”) in the ratio K^+/π^+ observed around beam energy 20–30A GeV [6], which has been discussed in the statistical model in Ref. [44]. Figure 7 shows the experimental peak as a function of $\sqrt{s_{NN}}$ along with the statistical model prediction calculated by means of the interpolations (15)–(20) and taking $A = 208$ along the curve. The theoretical error band corresponds to the 1σ ($\simeq 68\%$) six-dimensional ellipsoidal contour of the multivariate Gaussian distribution relevant to the six free parameters in our interpolating relations (15), (17), (20) (that is, T_0 , b , α , β , ζ , and ξ). In practice, this band has been

determined through a Monte Carlo procedure by randomly extracting 1000 times these parameters within the above contour and calculating, for each set, the K^+/π^+ ratio; the resulting minimum and maximum ratios were taken as the band bounds. The smooth interpolation of the SHM(γ_S) parameters fails to reproduce the horn because the model (see Table III) underestimates K^+ multiplicity at each energy point over the relevant range, especially at 20A and 30A GeV, where the discrepancy is of the order of 3 standard deviations. Pion multiplicities are also underestimated, but deviations are much less strong, especially at lower energies. In Fig. 7, the corresponding $\langle K^- \rangle / \langle \pi^- \rangle$ ratio is shown as well. In Pb-Pb collisions, the statistical model tends to overestimate this ratio because K^- multiplicities are relatively well reproduced at all beam energies, but the π^- multiplicities are underestimated, especially at the higher energies.

There are many possible reasons for this and other observed discrepancies, such as

- (i) A failure of the SHM(γ_S) scheme
- (ii) An insufficient knowledge of the hadronic mass spectrum and branching ratios
- (iii) An inadequacy of the assumptions needed to perform global fits, e.g., large fluctuations of charge distributions among the different clusters

As far as the first item is concerned, we observe that the most straightforward way of overcoming these difficulties is to add more parameters to the model, like the light-quark nonequilibrium parameter γ_q proposed in Ref. [45]. However, unlike γ_S , the introduction of this new parameter does not imply a remarkable and systematic improvement in the statistical model fits for all collisions [46]. In fact, by making a careful scan of a four-parameters fit at 20A GeV, in analysis A, we found that the best fit occurs at $\gamma_q = 0.7$, with $T \simeq 143$ MeV, $\mu_B/T \simeq 3.5$ with a $\chi^2/\text{dof} = 14.7/4$, i.e., only 0.8/4 units/dof less than the fit for $\gamma_q = 1$. On the other hand, at 30A GeV, we obtain a better fit ($\chi^2/\text{dof} = 9.5/4$ instead of 16.5/4) at $\gamma_q = 1.7$ with $T \simeq 124$ MeV and $\mu_B/T \simeq 3$, in agreement with Ref. [9], at a price of an abrupt change of γ_q about 1 and a decrease (contrary to the general trend) of temperature of 20 MeV within a range of only 1.4 GeV in center-of-mass energy. Such rapid changes might be simply due to random fluctuations generated by data overfitting, and they definitely need further investigations.

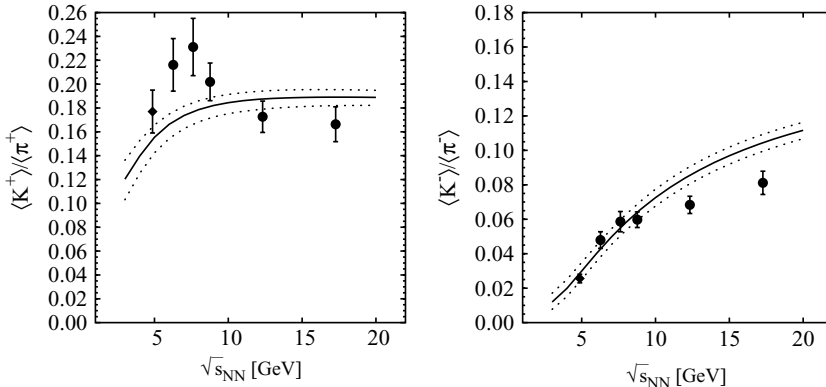


FIG. 7. Experimental vs interpolated $\langle K^+ \rangle / \langle \pi^+ \rangle$ ratios and $\langle K^- \rangle / \langle \pi^- \rangle$ ratios in central heavy ion collisions as a function of $\sqrt{s_{NN}}$. The “horn” structure around $\sqrt{s_{NN}} \sim 7\text{--}8$ GeV is clearly visible. The bands have been calculated by using a statistical model interpolating Eqs. (15), (17), and (20) with their central best-fit parameters and errors (see text).

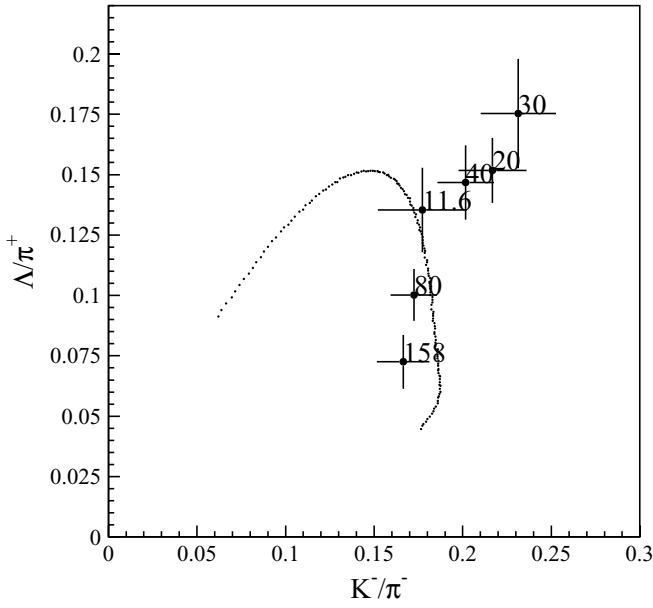


FIG. 8. Λ/π^+ vs K^-/π^- ratios measured in Pb-Pb and Au-Au collisions at various beam energies. Dashed line shows the central predicted values of the interpolations (15) and (16) with their best-fit parameters.

Concerning the second item, it should be emphasized that $\sim 70\%$ of π^\pm and $\sim 50\%$ of K^- multiplicities originate from resonance decays, while for K^+ the contribution increases from 25% at AGS to $\sim 50\%$ at RHIC. Although the uncertainty on the measured branching ratios do not play a significant role (see discussion in Sec. III), the possible presence of many undetected resonances may affect the calculation of final yields. One of the most remarkable examples is the σ scalar resonance, which is usually not included in these analyses. In fact, if the mass was 600 MeV and width 300 MeV, its inclusion

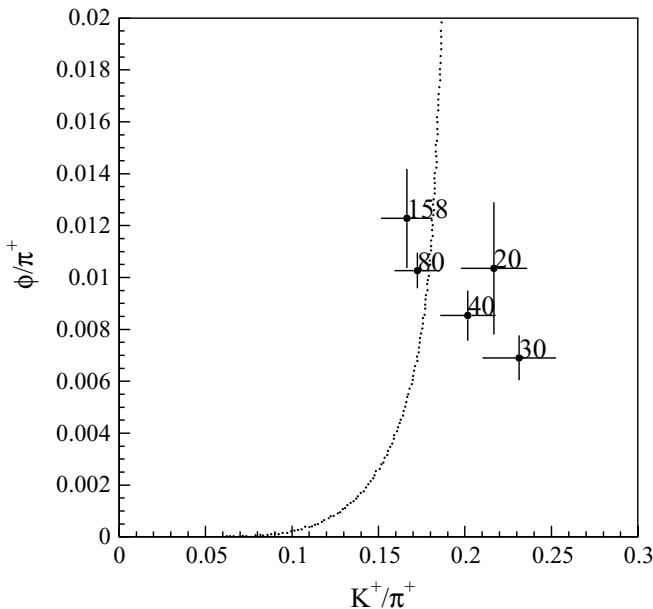


FIG. 9. Same as Fig. 8, but for ϕ/π^+ vs K^+/π^+ ratios.

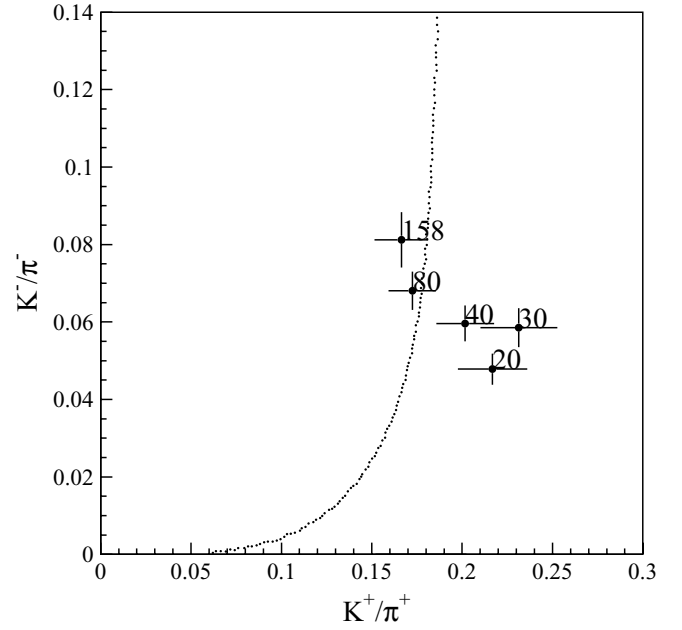


FIG. 10. Same as Fig. 8, but for K^+/π^+ vs K^-/π^- ratios.

would entail an enhancement of charged pion yield by about 20 units in Pb-Pb collisions at $\sqrt{s_{NN}} = 17.2$ GeV, which would make our fit better. However, it is difficult to conclude that the inclusion of this resonance would restore a perfect agreement with the data with still such a large uncertainty in its parameters.

Altogether, we deem that among the above proposed explanations of the observed discrepancies, the third one is the most conservative. Nonstatistical fluctuations of strangeness or baryon density, like those discussed, e.g., in Ref. [47], may invalidate the EGC assumption, thus affecting the global fit to particle multiplicities. Yet, such alternative pictures still need to be probed with a thorough comparison with the data.

The collisions between 20A and 40A GeV of beam energy are those showing the most significant discrepancies from the smooth SHM interpolations. This can be seen in Figs. 8–9 and 10, where the correlations between different particle ratios are shown along with the predicted central values of the interpolations (15), (16), and (20) as smooth dashed lines. All of these ratios involve strangeness-carrying particles, which may suggest that a peculiar dynamical process involving strange quarks occurs around this energy region.

VI. SUMMARY AND CONCLUSIONS

We have analyzed the available hadronic multiplicities measured in central heavy ion collisions over an energy range $\sqrt{s_{NN}} = 4.5\text{--}17.2$ GeV within the statistical hadronization model. The thermal parameters of the source, baryon chemical potential and temperature, depend strongly on the N - N center-of-mass energy, but their behavior is found to be smooth, and we have been able to find empirical relations describing their dependence on energy up to the top RHIC energy. Conversely, at fixed energy, they depend little on the system size, as we

have found similar values for μ_B and T at chemical freeze-out for C-C, Si-Si, and Pb-Pb.

On the other hand, chemical equilibration of strangeness is seen to be more dependent on the number of colliding nucleons than on energy, with the general trend for the strangeness under-saturation parameter γ_S to attain the value 1 only at energies $\sqrt{s_{NN}} = \mathcal{O}(100)$ GeV. Different versions of the SHM, aiming at explaining the observed under-saturation of the strange particle phase space, namely, the two-component model described here and strangeness correlation volume model examined in [7], seem to be disfavored by the data.

Discrepancies between the model with a strangeness under-saturation parameter and the data have been pointed out with regard to specific particle ratios. The origin of these discrepancies, mostly in the beam energy region 20A to 40A GeV, is still to be investigated.

ACKNOWLEDGMENTS

This work was partly supported by the NordForsk (J.M.) and Virtual Institute of Strongly Interacting Matter (VI-146) of Helmholtz Association, Germany.

-
- [1] See e.g., U. W. Heinz, Nucl. Phys. **A661**, 140 (1999).
 - [2] F. Becattini, Z. Phys. C **69**, 485 (1996); F. Becattini and U. Heinz, *ibid.* **76**, 269 (1997); F. Becattini and G. Passaleva, Eur. Phys. J. C **23**, 551 (2002); F. Becattini, Nucl. Phys. **A702**, 336 (2002).
 - [3] R. Hagedorn, in CERN Lectures on *Thermodynamics of Strong Interactions*, 1970; CERN-TH 7190/94, in *Hot Hadronic Matter*, edited by J. Letessier, H. H. Gutbod, and J. Rafelski (Plenum, New York, 1995), p. 13; R. Stock, Phys. Lett. **B456**, 277 (1999).
 - [4] M. van Leeuwen *et al.* (NA49 Collaboration), Nucl. Phys. **A715**, 161c (2003).
 - [5] M. Gazdzicki and M. I. Gorenstein, Acta Phys. Polon. B **30**, 2705 (1999).
 - [6] M. Gazdzicki *et al.* (NA49 Collaboration), J. Phys. G **30**, S701 (2004).
 - [7] F. Becattini, M. Gazdzicki, A. Keränen, J. Manninen, and R. Stock, Phys. Rev. C **69**, 024905 (2004).
 - [8] C. Alt *et al.* (NA49 Collaboration), Phys. Rev. Lett. **94**, 052301 (2005).
 - [9] J. Letessier and J. Rafelski, nucl-th/0504028, Phys. Rev. C (to be published).
 - [10] P. Braun-Munzinger, I. Heppe, and J. Stachel, Phys. Lett. **B465**, 15 (1999).
 - [11] C. Blume (NA49 Collaboration), in Proceedings of 40th Rencontres de Moriond, March 2005, hep-ph/0505137.
 - [12] I. G. Bearden *et al.* (BRAHMS Collaboration), Phys. Rev. Lett. **94**, 162301 (2005).
 - [13] I. G. Bearden *et al.* (BRAHMS Collaboration), Phys. Rev. Lett. **90**, 102301 (2003).
 - [14] S. Eidelman *et al.*, Phys. Lett. **B592**, 1 (2004).
 - [15] S. V. Afanasev *et al.* (NA49 Collaboration), Phys. Lett. **B491**, 59 (2000); J. Bachler *et al.* (NA49 Collaboration), Nucl. Phys. **A661**, 45 (1999); D. Barna (NA49 Collaboration), Ph.D. thesis, University of Budapest, 2004; S. V. Afanasev *et al.* (NA49 Collaboration), J. Phys. G **27**, 367 (2001).
 - [16] I. Kraus (NA49 Collaboration), J. Phys. G **31**, S147 (2005).
 - [17] L. Ahle *et al.* (E-802 Collaboration), Phys. Rev. C **60**, 044904 (1999).
 - [18] C. Alt *et al.* (NA49 Collaboration), J. Phys. G **30**, S119 (2004).
 - [19] L. Ahle *et al.* (E-802 Collaboration), Phys. Rev. C **59**, 2173 (1991).
 - [20] F. Becattini, J. Cleymans, A. Keränen, E. Suhonen, and K. Redlich, Phys. Rev. C **64**, 024901 (2001).
 - [21] S. Ahmad *et al.*, Phys. Lett. **B382**, 35 (1996).
 - [22] S. Albergo *et al.*, Phys. Rev. Lett. **88**, 062301 (2002).
 - [23] A. Richard (NA49 Collaboration), J. Phys. G **31**, S155 (2005).
 - [24] C. Blume (NA49 Collaboration), J. Phys. G **31**, S685 (2005).
 - [25] L. Ahle *et al.* (E802 Collaboration), Phys. Rev. C **60**, 064901 (1999).
 - [26] S. V. Afanasev *et al.* (NA49 Collaboration), Phys. Lett. **B491**, 59 (2000); **B538**, 275 (2002); Phys. Rev. C **66**, 054902 (2002).
 - [27] T. Anticic *et al.*, Phys. Rev. Lett. **93**, 022302 (2004).
 - [28] C. Meurer *et al.* (NA49 Collaboration), J. Phys. G **30**, S1325 (2004).
 - [29] C. Alt *et al.* (NA49 Collaboration), Phys. Rev. Lett. **94**, 192301 (2005).
 - [30] A. Mischke *et al.*, Nucl. Phys. **A715**, 453 (2003).
 - [31] V. Friese *et al.* (NA49 Collaboration), Nucl. Phys. **A698**, 487 (2002).
 - [32] S. Hamieh, K. Redlich, and A. Tounsi, Phys. Lett. **B486**, 61 (2000).
 - [33] F. Becattini and G. Passaleva, Eur. Phys. J. C **23**, 551 (2002).
 - [34] F. Becattini and L. Ferroni, Eur. Phys. J. C **38**, 225 (2004).
 - [35] D. H. Rischke, M. I. Gorenstein, H. Stoecker, and W. Greiner, Z. Phys. C **51**, 485 (1991).
 - [36] C. Hohne, F. Puhlhofer, and R. Stock, arXiv:hep-ph/0507276.
 - [37] D. Miskovic, <http://www-linux.gsi.de/~misko/overlap/>
 - [38] J. Cleymans, B. Kämpfer, P. Steinberg, and S. Wheaton, hep-ph/0212335 (2002).
 - [39] F. Becattini, L. Maiani, F. Piccinini, A. D. Polosa, and V. Riquer, Phys. Lett. **B632**, 233 (2006).
 - [40] J. Cleymans and K. Redlich, Phys. Rev. Lett. **81**, 5284 (1998).
 - [41] P. Braun-Munzinger, D. Magestro, K. Redlich, and J. Stachel, Phys. Lett. **B518**, 41 (2001); W. Florkowski, W. Broniowski, and M. Michalec, Acta Phys. Polon. B **33**, 761 (2002).
 - [42] P. Braun-Munzinger, J. Cleymans, H. Oeschler, and K. Redlich, Nucl. Phys. **A697**, 902 (2002).
 - [43] J. Cleymans, B. Kämpfer, M. Kaneta, S. Wheaton, and N. Xu, Phys. Rev. C **71**, 054901 (2005).
 - [44] J. Cleymans, H. Oeschler, K. Redlich, and S. Wheaton, Phys. Lett. **B615**, 50 (2005).
 - [45] J. Letessier and J. Rafelski, Phys. Rev. C **59**, 947 (1999).
 - [46] F. Becattini, M. Gazdzicki, and J. Sollfrank, Eur. Phys. J. C **5**, 143 (1998).
 - [47] V. Koch, A. Majumder, and J. Randrup, Phys. Rev. C **72**, 064903 (2005).